Zhou *et al. Cancer Nanotechnology* (2023) 14:42
https://doi.org/10.1186/s12645-023-00192-9

Cancer Nanotechnology

RESEARCH Open Access

Role of p53/circRNA0085439/Ku70 axis in DNA damage response in lung cells exposed to ZnO nanoparticles: Involvement of epigenetic regulation

Meiling Zhou[1†], Liang Xiao[2†], Jing Jin[1], Yin Wang[1], Peiyu Guo[1], Jinhua Luo[1], Magdalena Skonieczna[3,4] and Ruixue Huang[1*]

†Meiling Zhou and Liang Xiao have contributed equally to this study

*Correspondence: huangruixue@csu.edu.cn

[1] Department of Occupational and Environmental Health, Xiangya School of Public Health, Central South University, Changsha 410078, Hunan Province, China
[2] Faculty of Naval Medicine, Naval Medical University (Second Military Medical University), Shanghai 200433, China
[3] Department of Systems Biology and Engineering, Silesian University of Technology, Institute of Automatic Control, Akademicka 16, 44-100 Gliwice, Poland
[4] Biotechnology Centre, Silesian University of Technology, Krzywoustego 8, 44-100 Gliwice, Poland

Abstract

Background: Nano-Zinc oxide (Nano-ZnO) has been increasingly applied in agriculture, industry and biomedicine. However, the genotoxic effects of Nano-ZnO and the underlying mechanisms remain incompletely clear.

Methods: Human bronchial epithelial cell line (HBE) was used to observe the effects of Nano-ZnO on DNA damage repair-related proteins and epithelial mesenchymal transition (EMT) by Western blotting. Then, CRISPR/cas9-based technique was used to create p53 knockout (p53-KO) cell line. RNA-seq analysis was performed to uncover the circular RNA (circRNA) profile after Nano-ZnO treatment in p53-KO cells compared with p53 wild-type (p53-wt) cells. LC–MS/MS was used to discover the potential binding proteins of circRNA_0085439 in the p53 deficiency background after Nano-ZnO treatment. Nano-ZnO-induced DNA damage and EMT were also investigated in vivo by instillation of Nano-ZnO (50 μg/mouse).

Results: Nano-ZnO exposure caused DNA damage and EMT at both in vitro and in vivo background, which was reflected by increased DNA damage associated proteins such as ATM and ATR and γ H2AX. p53 expression increased at the early stage post Nano-ZnO treatment decreased later. RNA-seq assay showed a highest increase of circRNA_0085439 expression in p53-KO cells compared with the p53-wt cells after Nano-ZnO exposure. Silencing of p53 expression promoted its translocation of circRNA_0085439 from cytoplasm to nucleus leading to the formation of circRNA_0085439/Ku70 complex resulting in the decreased expression of Ku70 protein. In addition, increased EMT markers, N-cadherin and Vimentin, was observed in lung epithelial cells and in mouse lungs at day 7 after Nano-ZnO exposure.

Conclusions: This study unraveled the epigenetic mechanisms underlying Nano-ZnO-induced DNA damage and EMT. The effect of Nano-ZnO-induced DNA damage through p53/circRNA_0085439/Ku70 pathway likely contribute to Nano-ZnO-induced cell cytotoxicity and apoptosis. Our findings will provide information to further elucidate the molecular mechanisms of Nano-ZnO-induced cytotoxicity and genotoxicity.

Keywords: DNA damage, p53, Nano-ZnO, circRNA

Introduction

Currently, the global applications of nano-materials in the biomedical field are being extensively studied. However, the subsequent toxicological response to nano-materials, in particularly, on DNA damage remains incompletely clear. Nano Zinc oxide (Nano-ZnO) is a typical and an important class of transition metal nanoparticles with increasing application in wide aspects of agriculture, industrial and medical due to its high bioavailability and excellent physicochemical properties (Pei, et al. 2022). Since that, the exposure to human is inevitable and increases the risk of human health and environmental pollution at both occupational and non-occupational background. Public raise greater concern on the threat of Nano-ZnO cytotoxicity as the Nano-ZnO can enter into the body through respiratory system. We and other groups have indicated that exposure to Nano-ZnO cause cell cycle dysregulation in lung cancer cells (Lei et al. 2022), lung inflammation (Wu et al. 2020) or cell death (Cui et al. 2019), and also induces DNA damage in mice lung (Wang et al. 2020). For instance, acute Nano-ZnO inhalation induces ROS accumulation, DNA damage not only in human lung cancer cells, liver cancer cells, human skin fibroblast cells (Chiang et al. 2012) but also in embryo-larval zebrafish (Zhao et al. 2013). However, the potential molecular mechanism of Nano-ZnO-induced DNA damage and additional lung normal cells' injury such as epithelial mesenchymal transition (EMT) are still unclear.

Circular RNAs (circRNAs), a class of covalently closed RNAs formed by a back-splicing reaction have emerged as a complex family of transcripts with essential biological features (Timoteo et al. 2020). For instance, the human bronchial epithelial cell line (HBE) exposure to copper would induce larger number of circRNAs expression alterations (Chen et al. 2022a), and exposure to fine particulate matter would increase circ_Cabin1 expression, resulting in the DNA damage via inhibition of non-homologous end-joining repair (Zeng, et al. 2021). As of the increasing evidence demonstrate that circRNAs have an important role in the regulation of cells fate in response to the external insults. Although, there are no relative reports on the effects of nanoparticles on circRNAs alterations. Hence, we raised the hypothesis from an epigenetic perspective that the change of circRNAs after Nano-ZnO exposure may potentially involve into the regulation of Nano-ZnO-induced DNA damage repair-related proteins and additional EMT process.

P53 protein, encoded by the TP53 gene, is a critical tumor suppressive protein in maintaining homeostatic functions and adaptation to the environmental insults (Capaccia, et al. 2022). Biologically, p53 is at the core of responses to a larger number of cellular stress insults, in which the DNA damage is the most and first stressor for p53 stabilization (Lindstrom et al. 2022). Environmental genotoxic stressors such as ionizing radiation and nanoparticles can induce the DNA damage response and p53 offers a biological barrier against tumor progression through the activation of cellular signaling network (Gorgoulis et al. 2005). P53 senses the severity of DNA damage, thereby, activate repair pathways, cell cycle arrest and apoptosis (Lindstrom et al. 2022). P53 also participates into the epigenetic regulation. Chen et al. demonstrated that circRNA(has_circ_0065214, circSCAP) could inhibit the malignance of non-small cell lung cancer through the activation of p53 signaling (Chen et al. 2022b). A recent review pointed out that p53 can bind with microRNAs to form complex in the cellular physiological stress responses

(Capaccia, et al. 2022). Our previous reportdemonstrated that p53 plays important roles in the responses of lung cancer cells treated with Nano-ZnO (Lei et al. 2022). We also reported the normal human lung bronchial epithelial cell line, HBE exhibited transcriptomic and metabolomics alterations after p53 knockout in response to the silica exposure (Ju et al. 2021). Thus, in this study, we continue to investigate whether Nano-ZnO exposure would cause DNA damage and EMT as well as the role of p53/circRNA/DNA damage repair protein pathway at both in vivo and in vitro background.

Results

Characterization of Nano-ZnO and Nano-SiO_2

In Fig. 1A, the particulate Nano-ZnO showed rectangle in shape using TEM detection (Fig. 1A). For Nano-ZnO, the average particle size of Nano-ZnO was 80–100 nm (Fig. 1A), the mean hydrodynamic size of Z-Average (d. nm) was 984.5 nm, the Zeta potential was 5.37 mV; whereas for Nano-SiO_2, the mean hydrodynamic size of

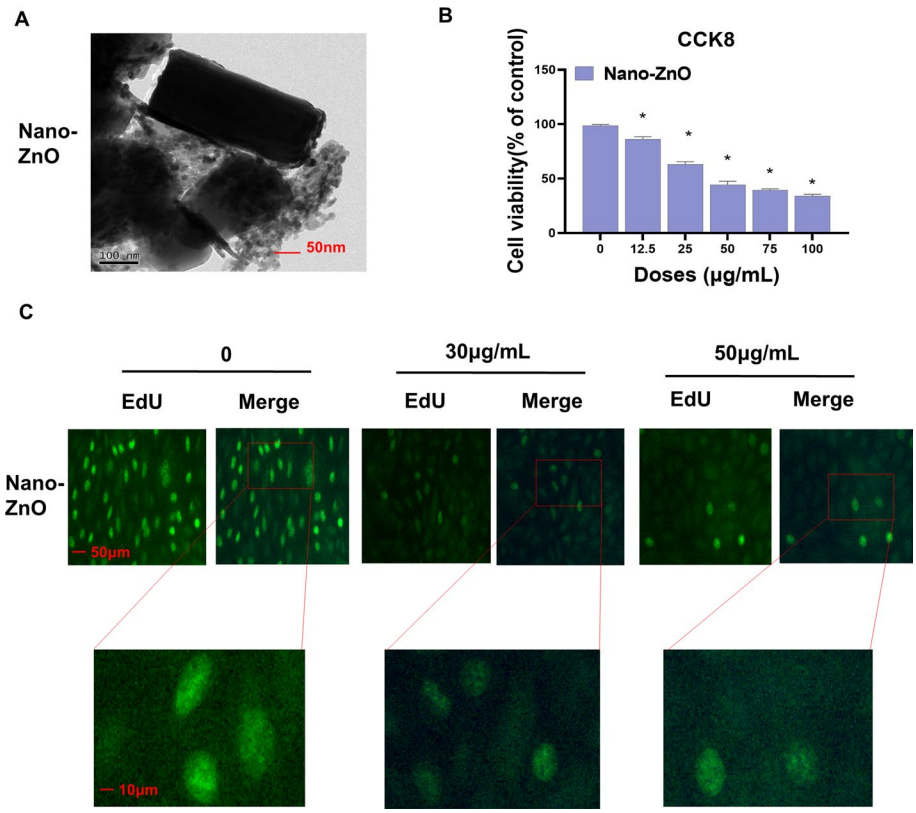

Fig. 1 Cytotoxicity of Nano particles on HBE cells. **A**. Characteristics of Nano-ZnO and Nano-SiO_2 by Transmission Electron Microscope (TEM). **B**. Cells were seeded in 96-well plates. After overnight culture, cells were treated with different concentration of nano particles for 24 h. Cells without nanoparticles treatment were used as the control. Cytotoxicity was determined by CCK8. **C**. The 5-Ethynyl–2′-deoxyuridine (EdU) positivity of HBE cells after different nanoparticles concentration treatment. Scale bar = 50 μm. Data were expressed as the mean ± SD. Differences between two groups were analyzed by t-test. When there were more than two groups, one-way analysis of variance (ANOVA) followed by Dunnett's post-hoc test was used for comparisons with the control. If there were two independent variables on a dependent variable, two way ANOVA followed by Holm-Sidak post-hoc test was employed. If necessary, transformation of data was used to achieve normally distributed data before analysis. A difference was considered statistically significant when a p-value was less than 0.05

Z-Average (d. nm) was 535.1, the Zeta potential was − 24.4 mV (Additional file 1: Fig. S1).

Nano-ZnO induced serious DNA damage in normal lung cells

Our previous study has affirmed that Nano-ZnO has roles in the regulation of lung cancer cells to affect the radiotherapy sensitivity (Lei et al. 2022), but the information about whether Nano-ZnO has adverse effect on normal lung epithelial cells is still insufficient. Exposure of normal lung cells HBE to Nano-ZnO at indicated concentrations up to 100 μg/mL for 24 h led to significant cell cytotoxicity measured by CCK8 assay (Fig. 1B). Moreover, the proportion of EdU positive cells decreased after treated with Nano-ZnO treatment (Fig. 1C). Apoptosis and cell cycle alterations in HBE cells after Nano-ZnO exposure were determined. Our results showed that Nano-ZnO markedly induced cell G2/M arrest (Fig. 2A, B), indicating the presence of potential DNA damage that HBE cells' normal repair process was affected. Furthermore, DNA damage was detected by comet assay. The results showed that the DNA tail moment in the cells treated with

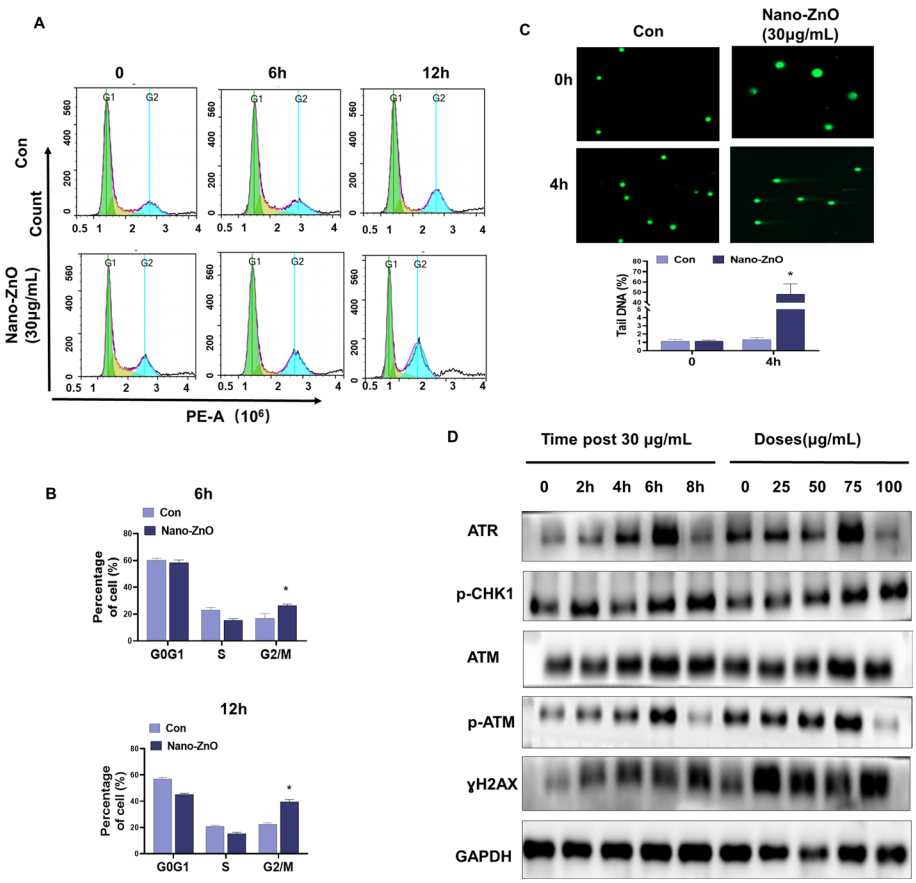

Fig. 2 Nano-ZnO exposure induced cell cycle G2/M arrest in HBE cells. **A**. Cell cycle assay at indicated time points between HBE cells treated with or without 30 μg/ml Nano-ZnO. **B**. Quantification of cell cycle distribution. **C**. Comet assay at 4 h after 30 μg/ml Nano-ZnO treatment in HBE cells. **D**. For the time-response study, cells were treated with 30 μg/mL of Nano-ZnO for 2, 4, 6, 8 h. For the dose–response study, cells were treated with 25, 50, 75, and 100 μg/mL of Nano-ZnO for 24 h. Cells without treatment were used as the "0". Nuclear protein was subjected to Western blot. ATR, p-CHK1, ATM, p-ATM and γH2AX were detected their proteins' expression. *Con* Control group

Nano-ZnO increased as compared with the control group (Fig. 2C). Expression of DNA damage response (DDR)-associated proteins in HBE cells post Nano-ZnO exposure was determined by Western blotting. Our results showed that Nano-ZnO upregulated ATR, p-CHK1 expression in a dose- and time-dependent manner (Fig. 2D). A dose- and time-dependent increase of γ H2AX and p-ATM were also observed after Nano-ZnO exposure, while the expression of total ATM was not affected by Nano-ZnO (Fig. 2E). It is known that phosphorylation ofγH2AX is a sensitive marker for DNA double strand breaks (DSBs), which could move to the damage site for recruiting other repair proteins (Huang and Zhou 2021). These results indicate that Nano-ZnO can induce DNA damage in normal lung cells.

Nano-ZnO exposure induced p53 accumulation, circRNAs profile alteration and down-regulation of DNA damage repair proteins

As of p53 has been identified to be essential protein in retaining genome stability and plays critical role in regulation of cell DNA damage repair-associated signaling pathway (Huang and Zhou 2020), we further explored the role of p53 in the cells post Nano-ZnO treatment. Figure 3A showed decreased expression of p53 and LIG4, a DNA damage repair protein after Nano-ZnO exposure. Considering p53 as a critical transcription factor, we knockout p53 expression (p53-KO)using CRISPR/cas9 to explore its role in the regulation of downstream molecules, in particular the circRNA by RNA-seq (Fig. 3B). The results showed with compared to p53 WT cells, 35 circRNAs up-regulated and 29 down-regulated in p53-KO cells after 30 μg/mL Nano-ZnO treatment (Fig. 3C, D). Bioinformatic analysis further showed that these changed circRNAs host genes may be enriched in the regulation of cell adhesion, protein binding (Fig. 3E) and signal transduction (Fig. 3F). These results indicated that after Nano-ZnO exposure, p53 expression decreased, DNA damage repair protein LIG4 decreased, and the decreased p53 may involve into regulation the epigenetic alteration of circRNAs in HBE cells.

Silencing of p53 increased circRNA_0085439 expression and promoted its translocation from cytoplasm to nucleus

CircRNA_0085439 was selected for further study due to its top increased expression level (Additional file 1: Table S1). To characterize circRNA_0085439, divergent primers were designed to amplify the circular transcripts, and convergent primers were used to detect the linear transcripts in both of cDNA and gDNA. The results showed circular form was amplified from cDNA but not gDNA (Fig. 4A, left gel, lane 1). We then investigated the association between p53 and circRNA_0085439. Total RNA was harvested at indicated time points and dosage slots. The results showed a time-and dose-dependent increase of circRNA_0085439 in p53-KO cells with compared to p53 WT cells (Fig. 4B, D). Immunofluorescence (IF) assay further showed that Nano-ZnO treatment in p53-KO cells increased the expression of circRNA_0085439 in nucleus whereas prior to Nano-ZnO treatment, circRNA_0085439 was present in cytoplasm (Fig. 4E). Moreover, silencing p53 increased ROS level in cells, which further identify that p53 KO induced cell damage after Nano-ZnO treatment (Fig. 5A). These results indicated that silencing of p53 promoted circRNA_0085439 higher expression and translocating it from cytoplasm to the nucleus.

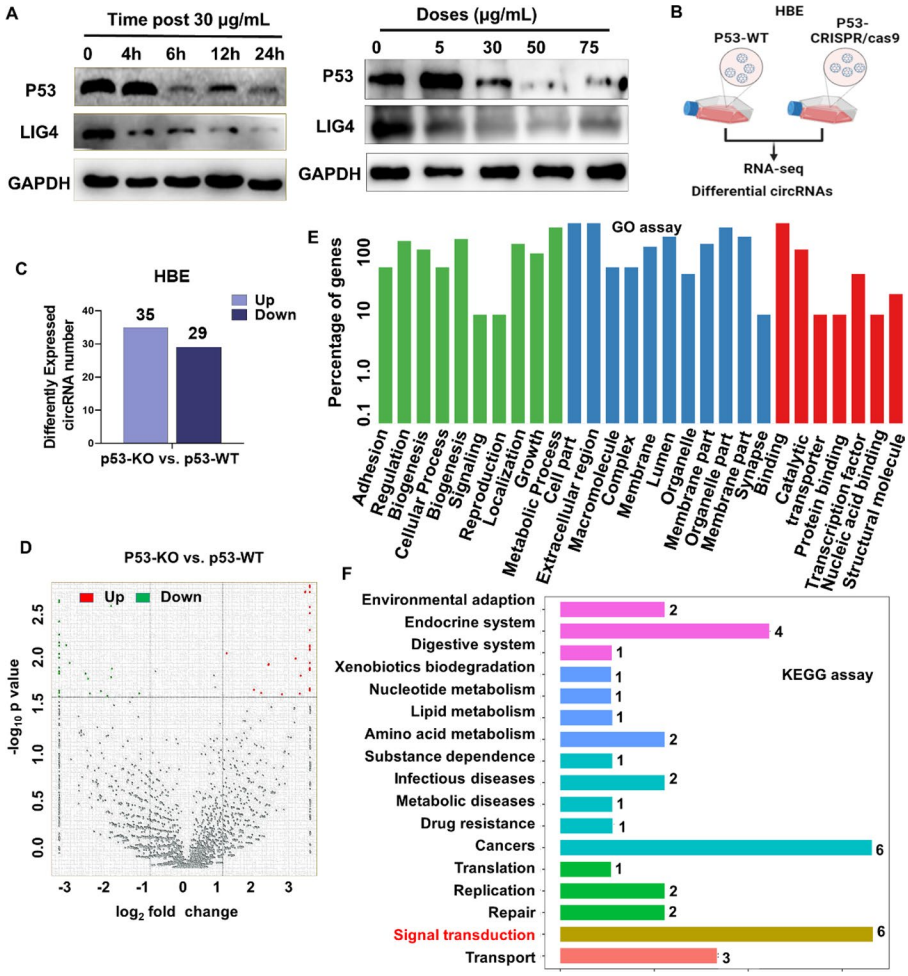

Fig. 3 Silencing of p53 cause circRNAs expression alterations in HBE cells after Nano-ZnO treatment. **A**. For the time-response study, cells were treated with 30 μg/mL of Nano-ZnO for 4, 6, 12 and 24 h. For the dose–response study, cells were treated with 5, 30, 50, and 75 μg/mL of Nano-ZnO for 24 h. Cells without treatment were used as the "0". Nuclear protein was subjected to Western blot analysis for the expression of. P53 and LIG4 proteins. **B**. For circRNAs RNA-seq assay, HBE cells were divided into p53-WTgroup and p53 knockout (p53-KO) group, after treatment with 30 μg/mL of Nano-ZnO for 24 h, cell were harvested and sent for RNA-seq. **C**. Numbers of up-regulated or down-regulated circRNAs in p53-KO cells compared with p53-WT cells after Nano-ZnO treatment. **D**. Volcano plot of up-regulated or down-regulated circRNAs in p53-KO cells compared with p53-WT cells after Nano-ZnO treatment. **E**. GO (Gene ontology) analysis was used to evaluate the changed circRNAs of its host genes' potential biological function. **F**. KEGG (Kyoto Encyclopedia of Genes and Genomes) analysis was used to evaluate the changed circRNA of its host genes' potential enriched pathway. 12 genes enrich to the signaling pathways related with cancer and signal transduction, 8 to the pathways related to amino acid metabolism, infectious diseases, replication and repair, 4 to the pathway of endocrine system. Data were expressed as the mean ± SD. Differences between two groups were analyzed by t-test

Silencing of p53 promoted circRNA_0085439 binding with Ku70

Given the circRNA_0085439 changes in p53-KO cells and translocation to the nucleus after Nano-ZnO treatment, we hypothesized that it may have potential for binding proteins to perform its biological function. To evaluate the biological function of circRNA_0085439, we generated a vector for efficient expression of circRNA_0085439 and silence its expression using siRNA sequence. We then divided p53-KO cells into

two groups, control group and circRNA_0085438 knockdown group, respectively. After Nano-ZnO treatment, both groups were conducted LC–MS/MS detection to find out the potential binding proteins with circRNA_0085439 (Fig. 5B). The potential binding proteins of circRNA_0085439 are listed in Additional file 1: Table S2. These potential binding proteins such as RBM39, HRNR, HSPA8 are significantly associated with different biological functions. Here, we selected the potential DNA damage-associated proteins for further study based on its higher fold change. As shown in Fig. 5B, in the p53-KO cells after Nano-ZnO treatment, silencing circRNA_0085439 increased Ku70 expression whereas overexpression of circRNA_0085439 decreased Ku70 expression (Fig. 5C). Other proteins were not affected by circRNA_0085439 after Nano-ZnO treatment. We then used RIP assay to confirm that circRNA_0085439 can bind with Ku70 to form the complex after Nano-ZnO treatment in the p53-KO cells (Fig. 5D). We used siRNA to silence p53 instantaneously in HBE cells and found silencing circRNA_0085439 increased Ku70 expression whereas overexpression of circRNA_0085439 decreased Ku70 expression (Fig. 5E). These results indicated that silencing p53 in normal lung cells resulted in the decrease of Ku70 protein expression through promoting circRNA_0085439/Ku70 binding complex formation.

Nano-ZnO induced lung epithelial mesenchymal transition (EMT)-related biomarkers' dysregulation in vivo and in vitro

It has been reported that Nano-ZnO induced N-cadherin increased in A549 cells (Martin and Sarkar 2019). Since N-cadherin is a critical biomarker to promote EMT process (Zhu et al. 2020), we hypothesized whether Nano-ZnO contributes to EMT-related biomarkers' dysregulation. Cells were divided into two groups, p53 WT group and p53-KO group. It is illustrated that the normal cell morphology was changed from round to long strip or spindle at 48 h after Nano-ZnO treatment, and in particular, more long strip condition was found in p53-KO cells compared with cells in p53 WT (Fig. 6A). Expression of EMT-associated proteins were detected by Western blotting. In p53-KO cells, the E-cadherin decreased whereas N-cadherin, Vimentin increased after Nano-ZnO treatment in a time-dependent manner (Fig. 6B).

C57BL/6 J mice were divided into two group, control group and Nano-ZnO group. Mice in Nano-ZnO group were intranasally instilled with 50 mg/kg/day per mouse of Nano-ZnO and lungs were collected at day 7 after exposure. HE staining illustrated that Nano-ZnO induced lung tissue damage, followed by interstitial inflammatory and cell infiltration and the pathological morphological changes (Fig. 7A). TEM observation present that Nano-ZnO enriched in the cells with the mitochondria crista of swelling, vacuoles and broken after Nano-ZnO treatment (Fig. 7B). Meanwhile, γH2AX increased and Ku70 decreased in mice lung tissues with Nano-ZnO treatment compared with control group (Fig. 7C). These data indicated that Nano-ZnO cause lung EMT in vivo and in vitro.

Discussion

Nano-ZnO is widely used as additive, photovoltaic devices and nano-mechanical components (Gilbert et al. 2012) and with prediction, the use of Nano-ZnO would continue to expand because of its unique chemical and physical characteristics. However, the

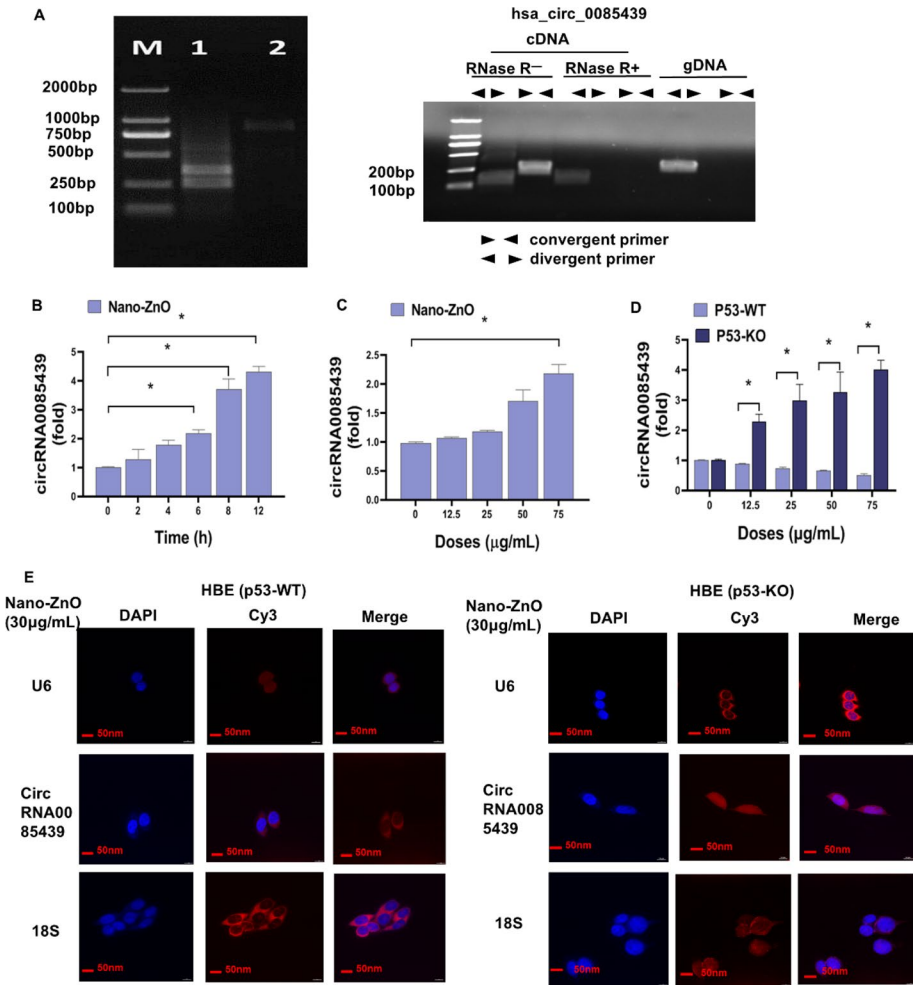

Fig. 4 Silencing p53 promoted circRNA_0085439 translocation from cytoplasm to nucleus after Nano-ZnO treatment. **A**. For left gel, the first 1 lane presents the RNA product fraction of circRNA_0085439 between 200 and 500 bp; while the second lane presents the size of production is between 700 and 1000 bp. For right gel, divergent primers were used to amplify circRNA_0085439 from cDNA but not genomic DNA (gDNA). Convergent primers amplified both of circRNA_0085439 and the linear GAPDH RNA in cDNA and gDNA. **B**. qRT-PCR was conducted to detect the circRNA_0085439 relative expression at indicated time points using μg/mL of Nano-ZnO. **C** and in both of p53 WT cells and p53-KO cells after different Nano-ZnO concentrations treatment (**D**). **E**. Representative images of circRNA_0085439 expression in p53 WT cells and p53-KO cells post 30 μg/mL of Nano-ZnO for 24 h analyzed by immunofluorescence. Nuclei were stained with 4,6-diamidino-2-phenylindole (DAPI). Data were expressed as the mean ± SD. Differences between two groups were analyzed by t-test. When there were more than two groups, one-way analysis of variance (ANOVA) followed by Dunnett's post-hoc test was used for comparisons with the control. If there were two independent variables on a dependent variable, two way ANOVA followed by Holm-Sidak post-hoc test was employed. If necessary, transformation of data was used to achieve normally distributed data before analysis. A difference was considered statistically significant when a p-value was less than 0.05

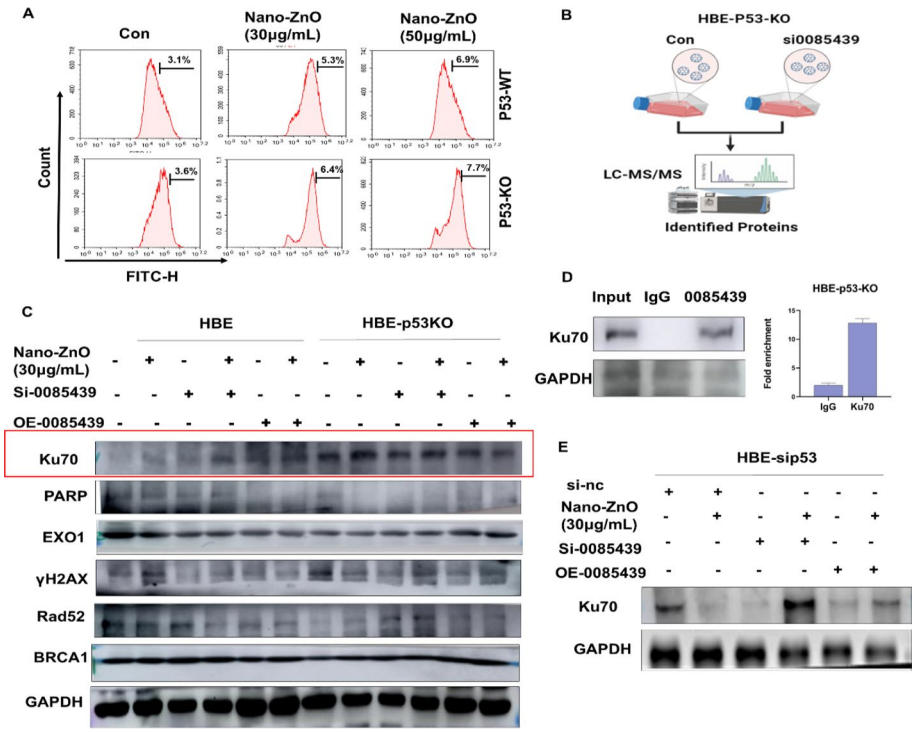

Fig. 5 Silencing p53 promoted circRNA_0085439/Ku70 complex formation post Nano-ZnO treatment. **A**. Flow cytometry analysis of intracellular ROS levels in p53 WT cells and p53-KO cells post 30 and 50 μg/mL of Nano-ZnO. **B**. Layout for the LC/MS/MS analysis of potential circRNA_0085439 binding proteins in p53 wild-type cells and p53-KO cells post 30 μg/mL of Nano-ZnO treatment. **C**. Expression of potential circRNA_0085439 binding DNA damage repair proteins in p53 wild-type cells and p53-KO cells post silencing circRNA_0085439 or overexpression circRNA_0085439 or post 30 μg/mL of Nano-ZnO treatment. **D**. RIP assay of the potential of circRNA_0085439 binding with Ku70 in p53-KO cells. **E**. Expression of potential circRNA_0085439 binding with Ku70 in cells treated with small interfering RNA p53 post silencing circRNA_0085439 or overexpression circRNA_0085439 or post 30 μg/mL of Nano-ZnO treatment. *si-nc* small interfering RNA-normal control, *OE* overexpression

increasing usage cause the increase risk of environmental and occupational exposure (Monse et al. 2018). It has reported that Nano-ZnO exhibit toxicity in human and other mammalian cell lines (Zaveri et al. 2010) as well as in soil and aquatic organisms (Fairbairn et al. 2011). Thus, it is important to deeply understand the toxic effects, in particular, the molecular mechanism of toxic effects on the respiratory cells.

DNA damage, which can be caused in response to a large amount of exogenous or endogenous insults includes a few types, such as DNA single-strand break and double-strand break compromises genome stability (Huang and Zhou 2021, 2020). Previous study has reported the Nano-ZnO-induced DNA damage in lung cancer cells such as A549 or H1299 cell lines (Lu et al. 2015). Here, in our study, we determined in vivo and in vitro Nano-ZnO-induced DNA damage in HBE normal lung cells and mice exposed to Nano-ZnO through intranasally instillation. As of the DNA damage elicits a series of DNA damage responses to occur, we detected some key proteins, p53, LIG4, ATM, γH2AX and ATR in order to confirm the role of Nano-ZnO in DNA damage of normal lung cells. It is known that γH2AX is an early signaling and biomarker for DNA damage repair and Nano-ZnO exposure can cause increase of γH2AX in murine embryonic stem cells (Karlsson et al. 2014). ATM activation may

modify a broad range of targets consisting of p53 and γH2AX via direct or indirect binding (Bourseguin et al. 2022). ATR activation may phosphorylate p53 leading to inhibition of cdc2 and cyclin B expression and induces G2/M arrest or inhibition of Bcl2 to induce apoptosis (Dok, et al. 2021). Li et al. compared four nanoparticles' cytotoxicity on BEAS2B cells and found that Nano-ZnO induce most servere cytotoxicity in a dose- and time-dependent manner with compared to Nano-SiO_2, TiO_2 and CeO_2, respectively (Cui et al. 2019). Uzar et al.reported 25–100 μg/mL Nano-ZnO can cause significant DNA damage and cytotoxic activity in renal cells (Uzar et al. 2015). Our results are consistent with previous reports that exposure of normal human bronchial epithelial cells (HBE) to Nano-ZnO can induce greater expression of γH2AX, ATR, ATM. On the other hand, Nano-ZnO decreased LIG4 and Ku70 proteins, indicating Nano-ZnO exposure causes DNA damage in particular DNA double-strand break in HBE cells. Furthermore, the increased γH2AX expression was also observed in mice lungs post Nano-ZnO treatment.

The molecular mechanisms underlying Nano-ZnO-induced DNA damage have not yet clearly elucidated. Typically, oxidative stress has been suggested to be a main mechanism in murine embryonic stem cells (Karlsson et al. 2014), in kidney epithelial

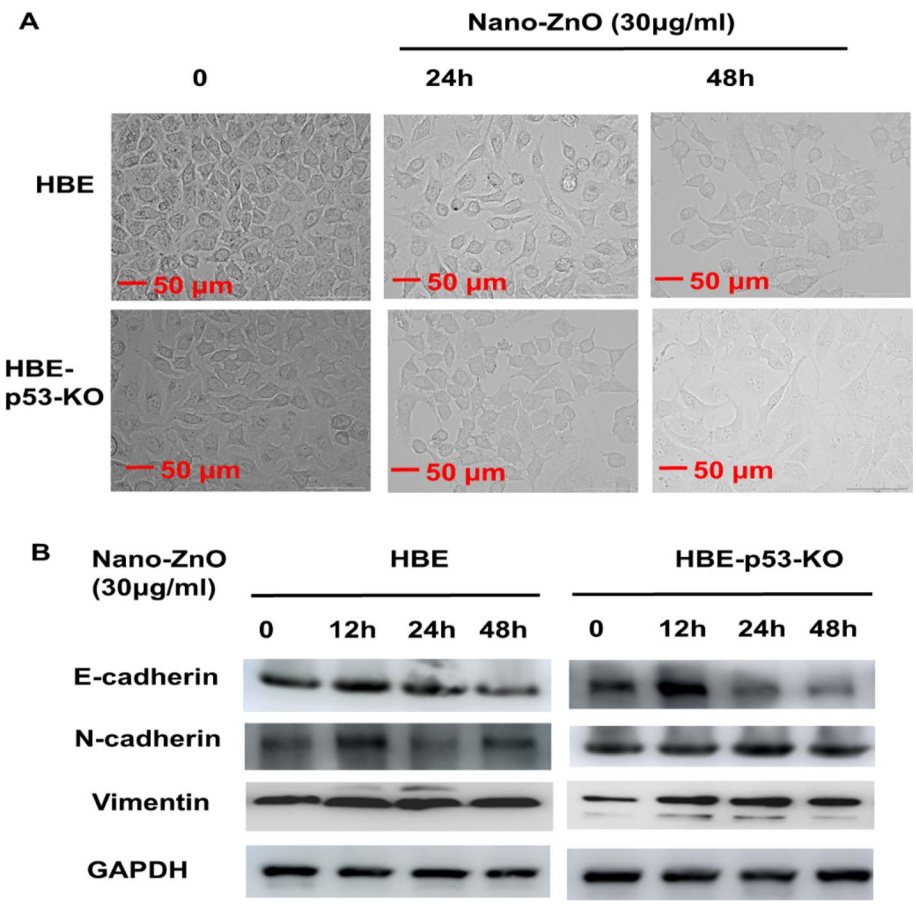

Fig. 6 Nano-ZnO exposure induced EMT. **A**. Exposure of Nano-ZnO (30 μg/mL) for 24 and 48 h in HBE cells with or without p53 presence. The cell morphology was took by light microscope. Scar bar: 50 μm. **B**. Nuclear protein was subjected to Western blot. E-cadherin, N-cadherin, and Vimentin were detected their proteins' expression

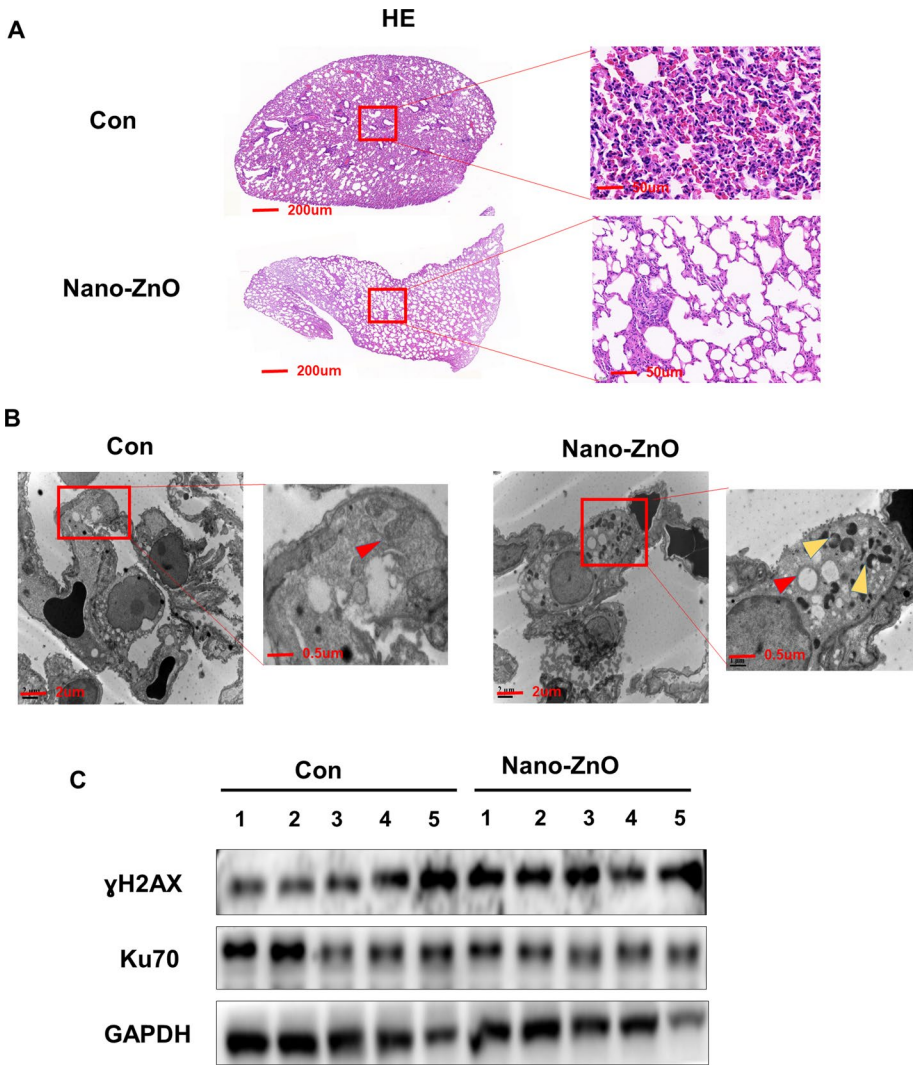

Fig. 7 Nano-ZnO exposure induced EMT in vivo. **A**. HE staining of mice lungs' pathology after 50 mg/kg/day installed per mouse of Nano-ZnO and lungs were collected at day 7 after exposure, Scar bar: 200 μm or 50 μm. **B**. TEM detection of mice lungs. Red arrows mean the mitochondrions while the yellow mean the nanoparticles. **C**. Nuclear protein was subjected to Western blot. γ H2AX and Ku70 were detected their proteins' expression

cells (Uzar et al. 2015), in liver cells (Yang et al. 2015) in "HaCat" keratinocytes (Wang et al. 2013) and in A549 cells (Chiang et al. 2012). Other mechanisms including increase of intracellular reactive oxygen species (ROS) (Zhang et al. 2018), ROS-triggered mitochondria-mediated apoptosis in zebrafish embryos (Zhao et al. 2016), induction of inflammatory reaction through increase of IL-1β, TNF-a and IL-6 in monocytes (Sahu et al. 2014). A study demonstrated that Nano-ZnO causes cytotoxicity through altering metabolism of amino acids, nucleotides, nucleosides and tricarboxylic acid cycle and elevation of DNA damage related toxic metabolites (Cui et al. 2019). Here, our study detected increased ROS generation after Nano-ZnO treatment in HBE cells which is consistent with previous study. Due to the very small size of Nano-ZnO, it may penetrate into the cell nucleus to interact with DNA double strand

to cause direct damage. Indeed, our study demonstrated that Nano-ZnO-phagocytized macrophages in mouse lungs. In addition, Nano-ZnO may induce DNA damage through indirect way to inhibit DNA damage repair ability which was confirmed in our study. We found decreased expression of LIG4 and Ku70, DNA damage repair-related key proteins in Nano-ZnO-exposed HBE cells and Nano-ZnO-instilled mouse lungs. The mechanistic understanding of Nano-ZnO-induced DNA damage remains in its infancy and needs to be further studied.

Recently, epigenetic-related mechanisms have been demonstrated that nano metal particles-induced DNA damage may be associated with epigenetic alterations such as involvement of microRNA (Mo et al. 2021; Abd-Rabou et al. 2021), long non-coding RNA (lncRNA) (Yan et al. 2021). For instance, Mo et al. indicated Nano-Ni activated expression level of HIF-alpha to increase miRNA-210 and decrease Rad52 to lead to the DNA damage in BEAS2B cells (Mo et al. 2021). Thai et al. indicated that exposure of silver nanoparticles induced alterations of mRNA and micRNA expression in human hepatocellular carcinoma cells (Thai et al. 2021). In this study, we also demonstrated that Nano-ZnO exposure caused dysregulation of p53/circRNA/Ku70 pathway (Fig. 8). In our study, firstly, Nano-ZnO exposure induced a trend of increase but later continuously decrease of p53 expression. This may due to that p53 expression is typically associated with different cell lines (Yang et al. 2021), different exposed concentrations (Chen et al. 2022c), different biological model (Zhao et al. 2016) and different Nano-ZnO chemical and physical properties (Thomas et al. 2022).

Our study showed that decrease of p53 promoted an increase in circRNA_0085439 expression after Nano-ZnO treatment in HBE and promoted circRNA_0085439 translocation from cytoplasm to nucleus, combining with Ku70 to form circRNA_0085439/Ku70 complex, and eventually inhibit DNA damage repair. CircRNA is a type of non-protein-coding RNAs that has a circular structure and do not possess a 5' cap or 3' poly-A tail. CirRNA has been reported to have ability to directly control mRNA homeostasis (Beltran et al. 2022). An increasing evidence has indicated that circRNA can regulate DNA damage repair-related pathway. Chen et al. found that circRNA_MTHFD1L can induce HR repair through miRNA/RPN6 axis resulting in the chemotherapy resistance in pancreatic ductal adenocarcinoma (Chen et al. 2022d). circRNA NIPBL can promote DNA damage in bronchial epithelial cells through the base excision repair pathway (Liu et al. 2022). We found here that Nano-ZnO treatment increased expression of circRNA_0085439 in p53 deficient cells. In addition, it has found that amount of circRNAs involved into the regulation of lung EMT process. Knockdown of circMAN1A2 could impede lung EMT (Dang et al. 2023), whereas overexpression of circPOLR1C could promote the EMT (Fang et al. 2022). These studies indicated the relationship between EMT and epigenetic regulation. Ku70 was identified as a circRNA_0085439 target; forced expression of circRNA_0085439 was able to suppress Ku70. circRNA_0085439 was found from WDR67 gene and mainly express in brain tissues (UCSC database, University of California Santa CruZ, https://genome.mdc-berlin.de/index.html) but less expression in other tissue parts. Study on circRNA_0085439 needs further efforts to discover its roles in nanoparticles insults in lung cells.

Ku70 has critical roles in non-homologous end joining (NHEJ) through activation of DNA-PKcs to recruit XRCC4-DNA ligase4-XLF complex formation for DNA damage repair (Lu et al. 2022), thereby preserving genomic integrity. Previous study has reported that nanoparticles can promote the ubiquitination of DNA repair protein Rad51 and promote the degradation of Rad51 to prevent the DNA repair (Xu et al. 2022). Nano-ZnO exposure leads to down-regulation of DNA repair protein Ku70 through increasing circRNA/Ku70 complex formation by silencing of p53 expression. The further mechanism underlying the circRNA/Ku70 in regulation of cellular response to Nano-ZnO needs to be explored.

In the current study, we found that Nano-ZnO exposure may cause normal human bronchial epithelial cells HBE to undergo EMT progress. Previous studies have reported that many kind of nanoparticles including nano graphene oxide (Zhu et al. 2020), gold nano-particles (Mo et al. 2019), Nano-TiO2 (Mo et al. 2019) may induce EMT. However, previous study did not perform experiment on promotion of EMT. Thus, in the real world, especially, the occupational population with long-term and continuous Nano-ZnO exposure such as industry of photocatalysts, gas sensors and biological fields should pay more attention on prevention control of health.

However, a few limitations of this study should be mentioned. First, the nanoparticlestoxicity evaluation is affected by many factors, in particular their sizes

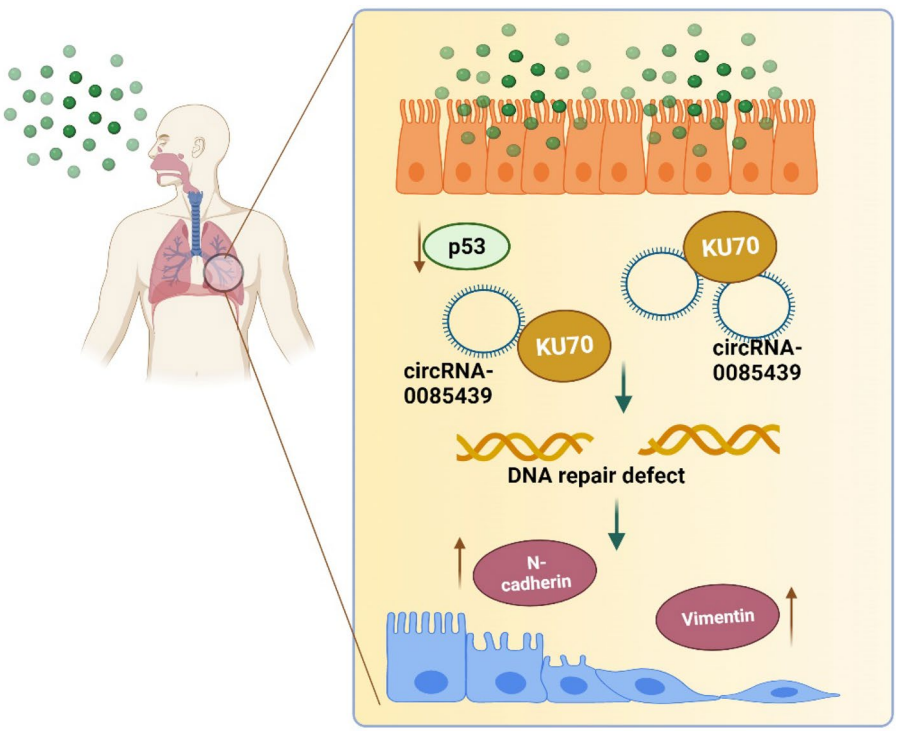

Fig. 8 Schematic diagram of the possible molecular mechanisms involved in Nano-ZnO-induced DNA damage and EMT. Briefly, Nano-ZnO causes cytotoxicity and DNA damage with decreased p53 expression and the DNA damage repair-related proteins. p53 silencing increased the circRNA_0085439 expression and the formation of circRNA_0085439/Ku70 complex, which decreased the Ku70 protein. DNA damage repair became defective. Moreover, the Nano-ZnO can cause EMT through decreasing E-cadherin and increasing N-cadherin and Vimentin expression levels

and physico-chemical properties, it is better to assess their toxicity in each property variant in vivo and in vitro. Second, only HBE cell line was used in the study, further study needs conducted on additional cell lines, such as BEAs2B and A549. Third, respiratory system is a very complex with not only the epithelial cells, but also endothelial cells and inflammatory cells, thus the exposure of Nano-ZnO may cause complex interactions of multiple cell types, but currently, we lack effectively methods to assay these interactions in vivo.

Conclusions

In summary, this study unraveled the molecular mechanism underlying Nano-ZnO-induced DNA damage and EMT. The effects of Nano-ZnO-induced DNA damage in normal lung epithelial cells through p53/circRNA_0085439/Ku70 pathway probably explain the cell damage from an epigenetic perspective. In addition, Nano-ZnO causes EMT through decreases of E-cadherin expression and increases of N-cadherin and Vimentin expression. Nano-ZnO-induced DNA damage in NHEJ repair may result in amounts of broken DNA fragments or base deletions, which needs to be further studied. Our finding will provide baseline information to further elucidate the underlying mechanism of Nano-ZnO-induced DNA damage and EMT.

Materials and Methods

Nano-ZnO preparation

The Nano-ZnO used in this study was purchased from Shanghai Macklin Biochemical Co., Ltd (CAS: 1314–13-2; Shanghai, China).The characteristics were described in our previous work (Lei et al. 2022). In this study, we detected the characteristics materials were consistent with our previous report Nano-ZnO was dispersed in physiological saline, ultrasonicated for 10 min in an FS30 ultrasonic cleaner (Fisher Scientific, Pittsburgh, PA), and vortexed thoroughly prior to each experiment. Briefly, the size and zeta potential were observed using a Malvern Zetasizer Nano ZS90. The photographs were obtained by transmission electron microscopy (TEM). Nano-ZnO was shipped to the Shiyanjia Laboratory (www.shiyanjia.com) for TEM, Z-Average and Zeta potential determination. The relative long-term stability of Nano-ZnO refers to the previous report (Han et al. 2011). For example, Nano-ZnO dose of 100 μg/ml was fixed as following details. We first weighed and suspended in deionized water at 10 mg/ml. then, the suspension was sonicated for 30 min in a water bath sonicator and after that, and appropriate stock solution was added to the cell culture medium to get the final suspension of dose at 100 μg/ml (Cui et al. 2019).

Chemicals, antibodies, and reagents

The antibodies used in this study were anti-Ecadherin (cat # 3195 s; dilution 1:1000 for Western blotting; Cell Signaling Technology), anti-N-Cadherin(cat # 13116 s; dilution 1:1000 for Western blotting; Cell Signaling Technology), anti-Vimentin (cat # 5741S; dilution 1:1000 for Western blotting; Cell Signaling Technology), anti-p53(cat # 2527S; dilution 1:1000 for Western blotting; Cell Signaling Technology), anti- γ H2AX (cat # 05–636; dilution 1:1000 for Western blotting), anti-ATR(cat # sc-515173; dilution 1:1000

for Western blotting; Santa Cruz Biotechnology), anti-p-CHK1(cat # 12302S; dilution 1:1000 for Western blotting and; Cell Signaling Technology), anti-ATM(cat # sc-377293; dilution 1:1000 for Western blotting; Santa Cruz Biotechnology), anti-p-ATM(cat # sc-47739; dilution 1:1000 for Western blotting; Santa Cruz Biotechnology), anti-LIG4(cat # 14649S; dilution 1:1000 for Western blotting; Cell Signaling Technology), anti-PARP (cat # 9532S; dilution 1:1000 for Western blotting; Cell Signaling Technology), anti-EXO1(cat # sc-56387; dilution 1:1000 for Western blotting; Santa Cruz Biotechnology), anti-Rad52 (cat # sc-365341; dilution 1:1000 for Western blotting; Santa Cruz Biotechnology). BRCA1 (cat # ab238983, dilution 1:1000 for Western blotting; Abcam).

CRISPR/cas9 technical was used to create p53-knockout (p53-KO) HBE cells. The details of creation steps are presented in our previous reports (Ju et al. 2021; Huang et al. 2020). Primer information for circRNA_0085439 was as follows: convergent primer, F: CGATGAAGGAATTAGCTC, R:GGCTGCTGTACTCTCCCTTA, divergent primer, F: GAGTCTAATACGACTCACTATAGGGAGTA, R: AGTAGAGACAAGGTTTCA CCATGTTG. For siRNA_0085439, the sequence of circRNA0085439 is: F-AAAAGA AUUAUAGUGAACATT, R-UGUUCACUAUAAUUCUUUUTT. pcDNA3.1-GFP was used to obtain the overexpression of the cloned plasmid of circRNA0085439 by GeneP-harma Ltd. Shanghai, China. The circRNA0085439 is 1132 bp length and the clone site is BamHI EcoRI.

Cell lines, small-interfering RNAs (siRNA) transfection and nanoparticle treatment

Human HBE cell line was purchased from the American Type Culture Collection (ATCC, Manassas, VA, USA) and cultured in Dulbecco's modified Eagle's medium supplemented with 10% foetal bovine serum, 100 μg/mL streptomycin, and 100 U/mL penicillin in a humidified 5% CO_2 atmosphere at 37 °C. The cells were treated with Nano ZnO ranging from 0, 12.5, 25, 50, 75, 100 μg/mL at room temperature for indicated time points. Based on this pilot dose–response experiments, the 30 μg/mL was selected for the following study. SiRNA transfection study was conducted as follows. Briefly, SiRNA duplexes were designed and synthesized by Shanghai GenePharma (Shanghai, China) and transfected into the cells using Lipofectamine 2000 (Thermo Fisher Scientific, Waltham, MA, USA) according to the manufacturer's instructions. Scrambled SiRNA was used as a negative control. At 48 h after transfection, the cells were collected for further analyses.

Cell Counting Kit-8 (CCK8) assay

To explore the cell viability post nanoparticles treatment, CCk8 assay was performed. The cells were seeded in 96-well plates at a density of 1×10^3/well. Each plate was used to analyze the cell proliferation by adding 10 μL CCK-8 (Sungene Biotech) solution at an interval of 12 h, up to 48 h.The absorbance of the samples at 450 nm were recorded. Data were presented as means ± SD of at least three independent experiments.

Comet assay

The DNA damage induced by Nano-ZnO was performed by Single cell gel electrophoresis kit (Biolab, China). HBE cells were collected and resuspended in PBS. 20 μL of the cells suspension and 80 μL of low melting agarose were mixed and 80 μL of the suspension pipetted onto a comet-slide. The slides were electrophoresed at low voltage

(300 mA, 25 V) for 30 min. Slides were removed from the electrophoresis unit after the designated time, tapped to remove excess buffer at room temperature. Subsequently, the air-dried slides were stained with DNA-binding dye propidium iodide (PI) and evaluated under a fluorescence microscope (Olympus IX81, Japan). The data were analyzed by CASP software based on 100 randomly selected cells per sample. The percentage of tail DNA, tail length and Olive tail moment (OTM) were selected as indicators of DNA damage. A total of 50 cells were randomly selected and captured per sample at 100 × magnification and analysed using the Open Comet Image J available at http://www.cometbio.org/. Tail length, percentage of tail DNA, and Olive Tail Moment (OTM) were calculated for DNA damage assessment.

Quantitative real-time PCR (qRT-PCR)

mRNA expression was assessed using a qRT-PCR method. Firstly, total RNA extraction from cells were done using TRIzol reagent (Jingcai Bio., Xi'an, Shanxi, China). The relative expression of mRNA was quantified using SYBR green dye (TB Green Premix Ex Taq II). Specific primers were designed by Green Pharma (Shanghai, China). qRT-PCR was performed using the following program: 95 °C for 10 min, 95 °C for 15 s, and 60 °C for 1 min, for 40 cycles. The program was performed in a CFX96 Touch apparatus (Bio-Rad). The relative expression was calculated using the 2-ΔΔCT method. The primers for circRNA_00085439 was F-ATCAGGGAGAGTACAGCAGC, R: TGGTAATCGGAA GTGTTGTGA.

CircRNA RNase R

To confirm that the circRNA_0085439 cannot be digested, RNase R (R0301, GeneSeed, Ltd., China) was used for RNA digestion to identify the circRNAs. Briefly, total RNAwere extracted from cells and divided into two fractions. For RNase R digestion, 1 μg of RNA was treated with 2U of RNase R. For the control, 1 μg of RNA was mixed with an equal volume of RNase-free water. After treatment, qRT-PCR was used to assess the expression levels of circRNA0085439.

CircRNA microarray

To explore the alterations of circRNAs between p53 wild-type control group and p53-knockout group, circRNA microarray (Arraystar Human circRNAs chip, ArrayStar) containing more than 5000 probes specific for splice sites in human circRNAs was used in this study provided by OEbiotech Bio-Tech Inc (https://www.oebiotech.com/). R software was used to process the subsequent data after quantile normalization. Differentially expressed circRNAs were identified through volcano plot filtering and fold change filtering. circRNAs with a fold.change ≥ 2.0 or ≤ 0.5 and a P-value < 0.05 were identified as significantly differentially expressed circRNAs. Relative bioinformatics was performed through GO assay and KEGG assay.

EdU assay

To explore the cell proliferation and DNA synthesis in HBE cells post Nano-SiO_2 or Nano ZnO treatments, the thymidine analog EdU (5-ethynyl-2'-deoxyuridine) assay

was conducted using a BeyoClickTM EDU Cell Proliferation Kit with Alexa Fluor 488(Cat#C0071S, Beyotime, China) according to the manufacturer's instructions. Briefly, the cells were seeded on confocal dishes at 1×10^5 cells/dish and cultured to reach a normal growth state. After the cells were treated with indicated Nano-ZnO concentrations (30, 50 μg/mL), DNA that carried integration of the synthetic nucleotide EdU was observed by Crestoptics X-Light V3 (Crest Optics, NIKON, Japan) confocal microscope. EdU-positive cells were counted using Image J software (National Institutes of Health).

Cell cycle analyses, cell apoptosis and ROS detection

For cell cycle assay, cells were seeded in 35-mm culture dishes at a density of 70–80% per dish. Cells were incubated with or without 30 μg/mL Nano ZnO and harvested at various time points (0, 6 h after treatment). After the cells were harvested, they were treated with RNase A (50 μg/mL) and incubated at 37 °C for 30 min. Then, the cells were stained with propidium iodide solution (50 μg/mL), and the cell cycle distribution was analysed using flow cytometry (A00-1–1102; Beckman Coulter, Inc., Suzhou, China), as described in our previous study (Dai et al. 2020). For cell apoptosis assay, the Annexin V-FITC Apoptosis Detection Kit (Beyotime) was used according to the manufacturer's instruction using a NovoCyte 2060R flow cytometer (ACEA Biosciences Inc.). For reactive oxygen species (ROS) detection, cells were stained with 500 μM of DCHF-DA working solution for 30 min at 37 °C and analyzed for ROS using NovoCyte 2060R flow cytometer (ACEA Biosciences Inc.).

Western blotting

Protein extraction and western blotting were performed as described previously (Ju et al. 2021). Images were captured and assessed using the ChemiDoc XRS + system (Bio-Rad, Hercules, CA, USA). Protein expression was quantified using Image Lab software (ver. 6.1; Bio-Rad). At least three independent replicates were analyzed per sample.

Immunofluorescence staining and confocal laser microscopy

To explore the cellular localization of circRNA_0085439 prior and post Nano-ZnO treatment, immunofluorescence staining was conducted. First, cells were divided into two groups, p53-wt group and p53-KO group. Cells were hybridized with Cy3-labeled oligonucleotide probe complementary to circRNA0085439 at 37 °C overnight, washed in graded SCC solutions (4 × , 2 × , and 1 × SCC for 5 min each) at 42 °C and protected from light, and the nuclei were stained with a DAPI-containing blocker. The nuclei of control cells stained with 4',6-diamidino-2-phenylindole (DAPI) were blue, 18S-CY3 was used for cytoplasm control and U6 is distributed in the nucleus and was used as an internal reference. At 4 h after transfection, the cells were treated with Nano-ZnO (30 μg/mL) and 0.25% Triton X-100. After incubation with the circRNA_0085439 probe, the samples were visualized using an LSM 510 confocal laser scanning microscope (Carl Zeiss, Oberkochen, Germany).

The sequences of involved probes are as follows. For circRNA0085439 probe, the sequence is, F- GAATAATGTTCACTATAATTCTTTTTACTTTCAAAATCAC-3′. For 18S-CY3, the sequence is, CTTCCTTGGATGTGGTAGCCGTTTC, For

NC-CY3, the sequence is, TGCTTTGCACGGTAACGCCTGTTTT. All the probes were designed and produced by GenePharma Ltd. Shanghai, China.

RNA immunoprecipitation (RIP) assay

To explore the binding potential between circRNA_0085439 and Ku70, RIP assay was conducted using Magna RIP ^{TM}Kit (EMD Millipore Corporation, Germany) according to the instructions. Briefly, RIP lysis buffer containing 25 mM Tris–HCL pH7.4, 150 mM NaCL, 1 mM EDTA, 1% NP-40 and 5% glycerol with RNase inhibitor and DNase and protease inhibitor cocktail. After the genomic DNA was digested, lysates were further subjected to sonication. Supernatants cleared by centrifugation were incubated with the anti-Ku70 antibody or IgG overnight and protein beads were added for a further 4 h incubation. After washing the beads, immunocomplexes of Ku70 and RNAs were de-cross linked. The RNAs were purified using Trizol and ethanol precipitation and subjected to qPCR analysis.

LC–MS/MS analysis

To explore the potential binding proteins with circRNA_0085439, LC–MS/MS analysis was conducted. Cells were divided into two group: control group (Con) and siRNA0085439 group. After treatment with 30 μg/mL Nano-ZnO, the samples were sent for detection by BiotechPack Scientific., Ltd. China. The condition for LC–MS/MS is listed on the website of BiotechPack Scientific., Ltd. China (BiotechPack Scientific., Ltd. China).

Exposure of mice to Nano-ZnO particles

Male C57BL/6 mice were purchased at 6 weeks of age from the Hunan SJA Laboratory Animal Co., LTD, China. All of the mice were housed at the Animal Laboratory Division, Xiangya School of Public Health, Central South University, China. All animal procedures and testing were conducted according to the National Legislation and local guidelines of the Laboratory Animals Center at the Central South University. The study and research protocols were approved by the Institutional Animal Review Board of Central South University (2020sydw0110). In addition, all animals in the study were treated humanely with regard to the alleviation of suffering. All mice were maintained in a specific-pathogen-free (SPF) environment with controlled conditions of a 12 h light/dark cycle at 20–22 °C and 45 ± 5% humidity. After 1 week of acclimation, the mice were used for the study with the group design detailed below. The mice were divided into two groups, control group and Nano-ZnO treatment group. Mice in Nano-ZnO group were intranasally instilled with 50 mg/kg/day per mouse of Nano-ZnO and lungs were collected at day 7 after exposure based on previous study (Nazir et al. 2019; Wu et al. 2014; Jung, et al. 2021). HE staining, TEM observation and Western blotting were used for detection of relative values.

Statistical analyses

All data are reported as the means ± S.D, and a p value < 0.05 was considered statistically significant (Student's t test). A fold change ≥ 2.0 and p value < 0.05 indicated differential

mRNA expression. Unpaired numerical data were compared using the unpaired *t test (*two groups) or analysis of variance (more than two groups). Statistical analyses were performed using SPSS for Windows software (ver. 22.0; SPSS Inc., Chicago, IL, USA).

Supplementary Information

The online version contains supplementary material available at https://doi.org/10.1186/s12645-023-00192-9.

Additional file 1: **Figure S1**. A. The Zeta Distribution data and volume distribution data for Nano-ZnO. B. The zata potential and size distribution for Nano-ZnO. C. The Zeta Distribution data and volume distribution data for Nano-SiO_2. D. The zata potential and size distribution for Nano-SiO_2. **Table S1**. Differential expressed circRNAs in the p53-KO vs. p53-WT HBE cells post 30ug/ml Nano-ZnO. **Table S2**. Differential expressed proteins in the si0085439 vs. control group in HBE cells with p53-KO post 30ug/ml Nano-ZnO.

Acknowledgements
Not applicable.

Author contributions
RH: conceptualization, Methodology, Formal analysis, Investigation, critically revised final manuscript, Funding acquisition; JJ, LX: investigation, cell experiments, Formal analysis, wrote the draft of study; PYG, YW, MLZ and JHL: investigation, cell experiments, Formal analysis. MS: technical direction and critically polished the manuscript. All the authors read and approved the manuscript. Reproduced images were created by RH and the elements used was permitted by Biorender (https://biorender.com/). All author read and approved the final manuscript.

Funding
This study was supported by grants from the National Natural Science Foundation of China (Grant Nos. 82273581, 82073486, U1803124), Scientific research project of Hunan Health Committee (202112010058).

Data availability
The data are available from the corresponding author on reasonable request.

Declarations

Ethical approval and consent to participate
All animal procedures and testing were conducted according to the National Legislation and local guidelines of the Laboratory Animals Center at the Central South University. The study and research protocols were approved by the Institutional Animal Review Board of Central South University (2020sydw0110).

Consent for publication
Not applicable.

Competing interests
The authors declare no competing financial and non-financial interests.

Received: 10 September 2022 Accepted: 7 April 2023
Published online: 24 April 2023

References

Abd-Rabou AA et al (2021) Metformin-loaded lecithin nanoparticles induce colorectal cancer cytotoxicity via epigenetic modulation of noncoding RNAs. Mol Biol Rep 48(10):6805–6820
Beltran M, Rossi F, Bozzoni I (2022) CircZNF609 as a prototype to elucidate the biological function of circRNA-mRNA interactions. Mol Cell Oncol 9(1):2055939
Bourseguin J et al (2022) Persistent DNA damage associated with ATM kinase deficiency promotes microglial dysfunction. Nucleic Acids Res 50(5):2700–2718
Capaccia C et al (2022) The complex interaction between P53 and miRNAs joins new awareness in physiological stress responses. Cells. https://doi.org/10.3390/cells11101631
Chen Z et al (2022a) The involvement of copper, circular RNAs, and inflammatory cytokines in chronic respiratory disease. Chemosphere 303(Pt 2):135005
Chen D et al (2022b) CircSCAP interacts with SF3A3 to inhibit the malignance of non-small cell lung cancer by activating p53 signaling. J Exp Clin Cancer Res 41(1):120
Chen FC et al (2022c) Effect of nano zinc oxide on proliferation and toxicity of human gingival cells. Hum Exp Toxicol 41:9603271221080236
Chen ZW et al (2022d) Circular RNA circ-MTHFD1L induces HR repair to promote gemcitabine resistance via the miR-615-3p/RPN6 axis in pancreatic ductal adenocarcinoma. J Exp Clin Cancer Res 41(1):153
Chiang HM et al (2012) Nanoscale ZnO induces cytotoxicity and DNA damage in human cell lines and rat primary neuronal cells. J Nanosci Nanotechnol 12(3):2126–2135

Cui L et al (2019) Predictive metabolomic signatures for safety assessment of metal oxide nanoparticles. ACS Nano 13(11):13065–13082
Dai X et al (2020) A novel miR-0308-3p revealed by miRNA-seq of HBV-positive hepatocellular carcinoma suppresses cell proliferation and promotes G1/S arrest by targeting double CDK6/Cyclin D1 genes. Cell Biosci 10:24
Dang QQ et al (2023) CircMAN1A2 contributes to nasopharyngeal carcinoma progression via enhancing the ubiquitination of ATMIN through miR-135a-3p/UBR5 axis. Hum Cell 36(2):657–675
Di Timoteo G, Rossi F, Bozzoni I (2020) Circular RNAs in cell differentiation and development. Development. https://doi.org/10.1242/dev.182725
Dok R et al (2021) Effect of ATR inhibition in RT response of HPV-negative and HPV-positive head and neck cancers. Int J Mol Sci. https://doi.org/10.3390/ijms22041504
Fairbairn EA et al (2011) Metal oxide nanomaterials in seawater: linking physicochemical characteristics with biological response in sea urchin development. J Hazard Mater 192(3):1565–1571
Fang Y et al (2022) circPOLR1C promotes the development of esophageal cancer by adsorbing miR-361-3p and regulating cancer cell apoptosis and metastasis. J Oncol 2022:9124142
Gilbert B et al (2012) The fate of ZnO nanoparticles administered to human bronchial epithelial cells. ACS Nano 6(6):4921–4930
Gorgoulis VG et al (2005) Activation of the DNA damage checkpoint and genomic instability in human precancerous lesions. Nature 434(7035):907–913
Han D et al (2011) Nano-zinc oxide damages spatial cognition capability via over-enhanced long-term potentiation in hippocampus of Wistar rats. Int J Nanomedicine 6:1453–1461
Huang RX, Zhou PK (2020) DNA damage response signaling pathways and targets for radiotherapy sensitization in cancer. Signal Transduct Target Ther 5(1):60
Huang R, Zhou PK (2021) DNA damage repair: historical perspectives, mechanistic pathways and clinical translation for targeted cancer therapy. Signal Transduct Target Ther 6(1):254
Huang R et al (2020) Integrated analysis of transcriptomic and metabolomic profiling reveal the p53 associated pathways underlying the response to ionizing radiation in HBE cells. Cell Biosci 10:56
Ju Z et al (2021) Transcriptomic and metabolomic profiling reveal the p53-dependent benzeneacetic acid attenuation of silica-induced epithelial-mesenchymal transition in human bronchial epithelial cells. Cell Biosci 11(1):30
Jung A et al (2021) Effect of pulmonary inflammation by surface functionalization of zinc oxide nanoparticles. Toxics. https://doi.org/10.3390/toxics9120336
Karlsson HL et al (2014) Mechanism-based genotoxicity screening of metal oxide nanoparticles using the ToxTracker panel of reporter cell lines. Part Fibre Toxicol 11:41
Lei R et al (2022) Potential role of PRKCSH in lung cancer: bioinformatics analysis and a case study of Nano ZnO. Nanoscale 14(12):4495–4510
Lindstrom MS, Bartek J, Maya-Mendoza A (2022) p53 at the crossroad of DNA replication and ribosome biogenesis stress pathways. Cell Death Differ 29(5):972–982
Liu Y et al (2022) Circular RNA circNIPBL promotes NNK-induced DNA damage in bronchial epithelial cells via the base excision repair pathway. Arch Toxicol 96(7):2049–2065
Lu S et al (2015) Comparison of cellular toxicity caused by ambient ultrafine particles and engineered metal oxide nanoparticles. Part Fibre Toxicol 12:5
Lu H et al (2022) DNA-PKcs-dependent phosphorylation of RECQL4 promotes NHEJ by stabilizing the NHEJ machinery at DNA double-strand breaks. Nucleic Acids Res 50(10):5635–5651
Martin A, Sarkar A (2019) Epithelial to Mesenchymal transition, eIF2alpha phosphorylation and Hsp70 expression enable greater tolerance in A549 cells to TiO(2) over ZnO nanoparticles. Sci Rep 9(1):436
Mo Y et al (2019) Gold nano-particles (AuNPs) carrying miR-326 targets PDK1/AKT/c-myc axis in hepatocellular carcinoma. Artif Cells Nanomed Biotechnol 47(1):2830–2837
Mo Y et al (2021) Nickel nanoparticle-induced cell transformation: involvement of DNA damage and DNA repair defect through HIF-1alpha/miR-210/Rad52 pathway. J Nanobiotechnology 19(1):370
Monse C et al (2018) Concentration-dependent systemic response after inhalation of nano-sized zinc oxide particles in human volunteers. Part Fibre Toxicol 15(1):8
Nazir S et al (2019) Antileishmanial activity and cytotoxicity of ZnO-based nano-formulations. Int J Nanomedicine 14:7809–7822
Pei X et al (2022) Lethality of zinc oxide nanoparticles surpasses conventional zinc oxide via oxidative stress, mitochondrial damage and calcium overload: a comparative hepatotoxicity study. Int J Mol Sci. https://doi.org/10.3390/ijms23126724
Sahu D, Kannan GM, Vijayaraghavan R (2014) Size-dependent effect of zinc oxide on toxicity and inflammatory potential of human monocytes. J Toxicol Environ Health A 77(4):177–191
Thai SF et al (2021) Effects of silver nanoparticles and silver nitrate on mRNA and microRNA expression in human hepatocellular carcinoma cells (HepG2). J Nanosci Nanotechnol 21(11):5414–5428
Thomas S et al (2022) Synthesis and characterization of zinc oxide nanoparticles of solanum nigrum and its anticancer activity via the induction of apoptosis in cervical cancer. Biol Trace Elem Res 200(6):2684–2697
Uzar NK et al (2015) Zinc oxide nanoparticles induced cyto- and genotoxicity in kidney epithelial cells. Toxicol Mech Methods 25(4):334–339
Wang CC et al (2013) Phototoxicity of zinc oxide nanoparticles in HaCaT keratinocytes-generation of oxidative DNA damage during UVA and visible light irradiation. J Nanosci Nanotechnol 13(6):3880–3888
Wang P et al (2020) Effect of intratracheal instillation of ZnO nanoparticles on acute lung inflammation induced by lipopolysaccharides in mice. Toxicol Sci 173(2):373–386
Wu W et al (2014) Synergistic effect of bolus exposure to zinc oxide nanoparticles on bleomycin-induced secretion of pro-fibrotic cytokines without lasting fibrotic changes in murine lungs. Int J Mol Sci 16(1):660–676

Wu Z et al (2020) Inflammation increases susceptibility of human small airway epithelial cells to pneumonic nanotoxicity. Small 16(21):e2000963
Xu Q et al (2022) Inhibiting autophagy flux and DNA repair of tumor cells to boost radiotherapy of orthotopic glioblastoma. Biomaterials 280:121287
Yan Q et al (2021) Long non-coding RNA OIP5-AS1 inhibits the proliferation and migration of esophageal squamous carcinoma cells by targeting FOXD1/miR-30a-5p axis and the effect of micro- and nano-particles on targeting transfection system. J Biomed Nanotechnol 17(7):1380–1391
Yang X et al (2015) Endoplasmic reticulum stress and oxidative stress are involved in ZnO nanoparticle-induced hepatotoxicity. Toxicol Lett 234(1):40–49
Yang R et al (2021) Zinc oxide nanoparticles promotes liver cancer cell apoptosis through inducing autophagy and promoting p53. Eur Rev Med Pharmacol Sci 25(3):1557–1563
Zaveri TD et al (2010) Contributions of surface topography and cytotoxicity to the macrophage response to zinc oxide nanorods. Biomaterials 31(11):2999–3007
Zeng H et al (2021) Circular RNA circ_Cabin1 promotes DNA damage in multiple mouse organs via inhibition of non-homologous end-joining repair upon PM2.5 exposure. Arch Toxicol 95(10):3235–3251
Zhang Y et al (2018) Nano-metal oxides induce antimicrobial resistance via radical-mediated mutagenesis. Environ Int 121(Pt 2):1162–1171
Zhao X et al (2013) Acute ZnO nanoparticles exposure induces developmental toxicity, oxidative stress and DNA damage in embryo-larval zebrafish. Aquat Toxicol 136–137:49–59
Zhao X et al (2016) Zinc oxide nanoparticles induce oxidative DNA damage and ROS-triggered mitochondria-mediated apoptosis in zebrafish embryos. Aquat Toxicol 180:56–70
Zhu J et al (2020) Graphene oxide promotes cancer metastasis through associating with plasma membrane to promote TGF-beta signaling-dependent epithelial-mesenchymal transition. ACS Nano 14(1):818–827

Publisher's Note